

Accepted Manuscript

Mechanistic PBPK Modeling of the Dissolution and Food Effect of a BCS IV Compound – the Venetoclax Story

Arian Emami Riedmaier, David J. Lindley, Jeffrey A. Hall, Steven Castleberry, Russell T. Slade, Patricia Stuart, Robert A. Carr, Thomas B. Borchardt, Daniel A.J. Bow, Marjoleen Nijsen

PII: S0022-3549(17)30685-8

DOI: [10.1016/j.xphs.2017.09.027](https://doi.org/10.1016/j.xphs.2017.09.027)

Reference: XPHS 943

To appear in: *Journal of Pharmaceutical Sciences*

Received Date: 24 July 2017

Revised Date: 8 September 2017

Accepted Date: 18 September 2017

Please cite this article as: Emami Riedmaier A, Lindley DJ, Hall JA, Castleberry S, Slade RT, Stuart P, Carr RA, Borchardt TB, Bow DAJ, Nijsen M, Mechanistic PBPK Modeling of the Dissolution and Food Effect of a BCS IV Compound – the Venetoclax Story, *Journal of Pharmaceutical Sciences* (2017), doi: 10.1016/j.xphs.2017.09.027.

This is a PDF file of an unedited manuscript that has been accepted for publication. As a service to our customers we are providing this early version of the manuscript. The manuscript will undergo copyediting, typesetting, and review of the resulting proof before it is published in its final form. Please note that during the production process errors may be discovered which could affect the content, and all legal disclaimers that apply to the journal pertain.



Title**Mechanistic PBPK Modeling of the Dissolution and Food Effect of a BCS IV Compound – the Venetoclax Story**

Arian Emami Riedmaier¹, David J Lindley², Jeffrey A Hall², Steven Castleberry², Russell T Slade², Patricia Stuart¹, Robert A Carr¹, Thomas B Borchardt², Daniel A.J Bow¹, Marjoleen Nijsen¹

¹DMPK and Translational Modeling, AbbVie Inc., North Chicago, IL 60064, USA

²Drug Product Development, AbbVie Inc., North Chicago, IL 60064, USA

Corresponding author: Arian Emami Riedmaier

Address: Drug Metabolism and Pharmacokinetics, AbbVie Inc., 1 North Waukegan Road, North Chicago, IL 60064

E-mail: arian.emamiriedmaier@abbvie.com

Competing Interests Statement and Disclosures

All authors are employees of AbbVie. The design, study conduct, and financial support for this research were provided by AbbVie. AbbVie participated in the interpretation of data, review, and approval of the publication.

Funding: This work was supported by AbbVie Inc.

ACCEPTED MANUSCRIPT

Abstract

Purpose: Venetoclax, a selective B-cell lymphoma-2 inhibitor, is a biopharmaceutics classification system (BCS) class IV compound. The aim of this study was to develop a physiologically-based pharmacokinetic (PBPK) model to mechanistically describe absorption and disposition of an amorphous solid dispersion (ASD) formulation of venetoclax in humans.

Methods: A mechanistic PBPK model was developed incorporating measured amorphous solubility, dissolution, metabolism and plasma protein binding. A middle-out approach was used to define permeability. Model predictions of oral venetoclax pharmacokinetics were verified against clinical studies of fed and fasted healthy volunteers, and clinical drug interaction studies with strong CYP3A inhibitor (ketoconazole) and inducer (rifampicin).

Results: Model verification demonstrated accurate prediction of the observed food effect following a low-fat diet. Ratios of predicted versus observed C_{max} and AUC of venetoclax were within 0.8- to 1.25-fold of observed ratios for strong CYP3A inhibitor and inducer interactions, indicating that the venetoclax elimination pathway was correctly specified.

Conclusions: The verified venetoclax PBPK model is one of the first examples mechanistically capturing absorption, food effect and exposure of an ASD formulated compound. This model allows evaluation of untested drug-drug interactions, especially those primarily occurring in the intestine, and paves the way for future modeling of BCS IV compounds.

Keywords

Amorphous

ADME

Bioavailability

Food Effect

Physiologically based pharmacokinetic modeling

Clinical pharmacokinetics

Intestinal absorption

Passive diffusion/transport

Drug interaction

ACCEPTED MANUSCRIPT

Abbreviations

ASD - Amorphous Solid Dispersion

BCS – biopharmaceutics classification system

CLL – chronic lymphocytic leukemia

CYP – cytochrome P450

DLM – diffusion layer model

GLPS – glass-liquid phase separation

$P_{\text{eff.,man}}$ – effective permeability in human

PBPK – physiology based pharmacokinetics

PK - pharmacokinetic

SIVA - Simcyp In Vitro (data) Analysis

USP - United States Pharmacopeia

Introduction

Venetoclax is a selective and orally bioavailable B-cell lymphoma-2 inhibitor developed for the treatment of chronic lymphocytic leukemia (CLL) and other hematological malignancies^{1,2}. In the clinic, venetoclax has demonstrated efficacy as a single agent in patients with relapsed CLL or small lymphocytic lymphoma and as combination therapy in other hematological malignancies^{2,3}.

Venetoclax, a biopharmaceutics classification system (BCS) class IV compound, has low solubility (crystalline solid; < 4ng/mL) and permeability^{2,4,5}, which poses challenges to mechanistic modeling and formulation design, particularly with respect to understanding the fraction absorbed in the intestine. A drug in this class would be predicted to be both solubility and permeability-limited, thus making absorption highly dependent on *in vivo* relevant concentrations present from proximal (duodenum) to distal (colon) intestinal regions. Current physiologically-based pharmacokinetic (PBPK) modeling approaches have shown limited success in predicting absorption of BCS class IV compounds. A complicating factor for successful model development for this class of molecules is the tendency for the application of solubility-enabling or supersaturating formulations to enhance *in vivo* exposure. Utilization of the intrinsic crystalline solubility as the main formulation input to the model in these situations can result in significant under-predictions in absorption, as the concentration available in the supersaturated state is not fully taken into account. Therefore, an understanding of drug release and supersaturation maintenance as related to potential interactions in the intestine is critical to building an appropriate PBPK model with this type of formulation⁶⁻⁸.

Amorphous solid dispersions (ASDs) have emerged as a formulation approach to overcome the aqueous solubility limitations of poorly soluble drugs. In general, ASDs offer significant advantages over crystalline formulations as the apparent, amorphous solubility of a drug can be orders of magnitude higher than its crystalline counterpart^{9,10}. The increased solution concentration of the drug provided via its amorphous solubility has been demonstrated to drive flux through epithelial barriers present in the GI tract, typically resulting in higher overall exposures^{11,12}. A key factor limiting the utilization of ASDs is physical stability and the potential for crystallization of the drug upon generation of the metastable, supersaturated state in

aqueous solution. Drugs with higher molecular weight (such as venetoclax), tend to be slow crystallizers and can remain in the supersaturated state at the amorphous solubility across physiologically relevant time-frames in the presence of amorphous drug-rich particles, which serve as reservoirs of absorbable drug^{9,12}. Amorphous solubility as a PBPK model input will more accurately represent the free fraction of drug available in the gastrointestinal lumen than the more traditional approach of using crystalline solubility. To account for the role of pH along with bile salt and micelle concentrations on solubility across the gastrointestinal tract, amorphous solubility should not only be generated in a buffer to designate the maximal luminal free fraction concentrations, but also measured in biorelevant simulated intestinal fluids. Importantly, the resulting experimental amorphous solubility data should be input into a PBPK model that can apply appropriate total solubility enhancements across the gastrointestinal tract due to the presence of bile salts and other micellar structures ahead of subsequent modeling of absorption.

For venetoclax, measured *in vitro* solubility was compared to the predicted solubility (via the algorithms implemented in the PBPK platform) using the Simcyp *in vitro* (data) analysis (SIVA) toolkit 2.0 (Certara USA, Inc., Princeton, NJ) to define a scalar for the bile-micelle partition coefficient⁶. These scalars were then utilized within the Simcyp PBPK platform for predicting total biorelevant solubility. In addition to plasma protein binding, volume of distribution and measured enzyme kinetics, this data was used to predict and verify the *in vivo* pharmacokinetic (PK) profile of venetoclax, the impact of food and its potential drug interactions.

While a PBPK model has previously been used to describe the disposition of venetoclax using clinical dissolution data¹³, the aim of this work was to use *in vitro* data on solubility, dissolution and permeability to mechanistically capture the absorption, disposition and food effect of ASD venetoclax tablets.

Materials and Methods

Materials

DMSO, methanol and 50 mM phosphate buffer pH 7.4 (ionic strength = 0.155 M) and polyvinylpyrrolidone K40 were obtained from Sigma-Aldrich (St. Louis, MO). 0.1N HCl and Polysorbate 80 were obtained from

J.T. Baker (Phillipsburg, N.J.) Sodium chloride was obtained from Calbiochem (San Diego, CA). HPMC, Hypermellose 2910 was obtained from Spectrum (New Brunswick, NJ). HPMC-AS was obtained from Shin-Etsu (Tokyo, Japan). Kollidon VA64 (Copovidone) was obtained from BASF (Ludwigshafen, Germany). All simulated intestinal fluid powders were obtained from Biorelevant (London, UK). Lauroglycol FCC was obtained from Gattefosse and venetoclax API was manufactured by AbbVie (North Chicago, IL).

Human plasma was purchased from BioreclamationINV (Hicksville, New York). A 96-well equilibrium device (HTD 96C, high throughput dialysis device in a 96-well format), cellulose membranes with molecular weight cut-off (MWCO) of 12-14 kDa and adhesive plate sealers were purchased from HT-Dialysis (Gales Ferry, Connecticut). Deep well plates were obtained from Sales and Service (Flanders, New Jersey).

Methods

Unbound Fraction in Plasma ($f_{u,p}$)

The unbound fraction of venetoclax to human plasma was determined by equilibrium dialysis using a 96-well HT dialysis apparatus with dialysis membrane strips (MWCO 12-14 kDa). A generalized equilibrium dialysis method was adopted from literature¹⁴. Briefly, venetoclax (1-30 μ M in 1% (v/v) human plasma) was equilibrated against dialyzed phosphate buffer (50 mM, pH 7.4). Dialyzed buffer from human plasma was prepared by incubating naïve human plasma with phosphate buffer. Dialyzed buffer was on the buffer side of the membrane in the diluted human plasma studies. After the incubation (4 hr at 37 °C), matrix (5 μ L) and buffer (50 μ L) were sampled from the dialysis plate and combined with acetonitrile/methanol containing 50 nM carbutamide as the internal standard (quench solution). The 10-fold difference in sample volume from the dialysis plate allows the standard curve for buffer to be 10-fold lower. A standard curve and T_0 (time=0) samples were treated the same as the dialysis samples by matrix blanking. Samples were vortexed and stored at 4 °C, if necessary, prior to centrifugation and analysis by HPLC-MS/MS.

The extent of binding was determined by measuring the fraction unbound (f_u) of the test article. It is assumed that the unbound test article will equilibrate freely across the membrane and thus the concentration in the buffer chamber will be the free concentration (C_f). The free concentration divided by the total concentration is the fraction unbound:

$$f_u = \frac{C_f}{C_t} \quad (1)$$

where f_u is the fraction of unbound drug, C_f is the free concentration of test article and C_t is the total concentration of test article.

The unbound fraction in diluted plasma was back-calculated to undiluted plasma using the following equation:

$$\text{Undiluted } f_u = \frac{1/D}{\left(\frac{1}{f_{u,\text{measured}}}\right)^{-1} + 1/D} \quad (2)$$

where D represents the fold dilution of matrix, and $f_{u,\text{measured}}$ is the ratio of concentration determined from the buffer and diluted plasma samples¹⁵.

Intestinal Permeability

Sprague-Dawley rats (8 – 10 weeks old) were used for all studies. All animal procedures were approved by the Institutional Animal Care and Use Committee (IACUC) at AbbVie Inc. Intestines were removed immediately post-sacrifice via sharp dissection of the mesentery. The gut from stomach to colon was then placed in ice cold HEPES buffer (25 mM) for transport. Tissue was prepared for testing by first removing the segment 2 cm above attachment to the caecum to a length of approximately 10 cm, opening the intestine *via* dissection down the mesenteric attachment, followed by blunt dissection of the muscularis propria. Tissues were then mounted in the Ussing chamber apparatus (Physiologic Instruments; EM-CSYS-8) and monitored for integrity by online measurement of trans-epithelial electrical resistance; this measurement was continuously monitored throughout the study.

Permeability of venetoclax was measured using a 100 µg/mL GLPS-based formulation in a 1% copovidone solution in HEPES buffer at pH 7.2. In the basolateral receiver chamber, a 1% (w/v) BSA solution was used to collect permeated drug. The study was run for five hours; at each hour interval a 10 µL sample was collected from each basolateral compartment. Samples were analyzed via mass spectroscopy. Permeability calculated from a linear fit was applied to the accumulated drug concentration using the measured free drug concentration in the donor compartment. This permeability was then converted by an internal correlation of nine model compounds run in the Ussing chamber apparatus and published effective permeability values for human jejunum ($P_{eff,man}$)¹⁶ (Appendix 1).

Solubility and Dissolution

A concentrated stock solution was prepared by dissolving venetoclax in DMSO at a concentration of 50 or 100 mg/mL, sonicating if necessary to obtain a clear solution. The test medium of interest (0.5 mL) was added to a 15x45mm Type 1 Class B borosilicate glass vial (Sun-Sri). While mixing with a touch mixer, 5 µL of the concentrated stock solution was added to the vial. A portion of the supersaturated suspension (~0.18 mL) was transferred to an ultra-clear ultracentrifuge tube (5x20 mm, Beckman Coulter), placed in a Beckman Coulter A-110 fixed angle rotor and centrifuged at ~100,000 RPM in an Airfuge Ultracentrifuge (Beckman Coulter) for ~30 minutes. The remaining supersaturated sample was retained for analysis by cross-polarized light microscopy (Nikon Eclipse E600 POL Microscope). Amorphous solubility measurements were conducted in 50 mM phosphate buffer (pH 7.4) with 0.5% (w/v) copovidone or a cocktail of various polymers to inhibit crystallization and stabilize at the amorphous solubility. Additional amorphous solubility experiments were conducted in simulated intestinal fluids (FaSSIF and FeSSIF) at pH 5 and 6.5. The composition of FaSSIF is 3 mM sodium taurocholate and 0.75 mM lecithin with an osmolarity of 270 mOsmols. For FeSSIF, the composition is 5-fold this composition or 15 mM sodium taurocholate and 3.75 mM lecithin with the same osmolarity¹⁷.

To assess precipitation behavior of venetoclax, the samples described above were allowed to equilibrate at room temperature for 24 hours and a small sample of each suspension was pipetted onto a glass slide and viewed through a polarized light microscope and observed for birefringence/presence of crystalline particles.

***In vitro* Modeling of Solubility**

The bile to micelle solubilization of venetoclax was estimated using the Simcyp SIVA toolkit, version 2.0.19.0 (SIVA; Simcyp Ltd. Certara Inc). Briefly, SIVA is a parameter estimation tool that allows estimation of intrinsic solubility, pK_a , and micelle partition coefficients from experimentally determined pH-solubility profile and bio-relevant solubilities. Adjusting these parameters within the PBPK platform to obtain a “best fit” of the clinical PK profile could lead to a biased understanding of the relative contribution of these parameters due to the concomitant role of system- and drug-related variables that may additionally contribute to any observed *in vitro-in vivo* differences. Here, the experimental pK_a , calculated $\log P_{\text{octanol:water}}$ (using measured $\log D$ at pH 7.4)¹⁸, and the intrinsic amorphous solubility were fixed and the biorelevant solubility in FaSSIF and FeSSIF buffer were used in fitting and verification of the micelle to buffer partition coefficient ($\log K_{m,w}$) of venetoclax. Tables 1 and 2 provide a summary of the measured input parameters and final estimated solubility and absorption parameters that were used as input for the PBPK model.

Additional references (including details of methodology) and previously published input parameters used in the current PBPK model can be found in Table 2.

PBPK Model Development and Evaluation

The venetoclax PBPK model was built using the Simcyp® Simulator, Version 15.0.86.0 (Certara USA, Inc., Princeton, NJ). All simulations described in this study were carried out in the Sim-Healthy Volunteer population.

The PBPK model was developed using measured *in vitro* drug parameters as surrogates for *in vivo* mechanisms relevant to absorption, distribution and metabolism. The link from *in vitro* parameters to an *in vivo* context was established using *in vitro-in vivo* extrapolation through the use of inter-system extrapolation factors and systems scalars, as well as mechanistic integration of these parameters in the framework of the whole human body^{19,20}. An exception to this was the permeability in jejunum, where *in vitro-in vivo* extrapolation has not been established in the presence of efflux transporters due to differences in expression and activity across species. Therefore, jejunum permeability was refined based

on the observed clinical profile²⁰. All input drug parameters are summarized in Table 1 and 2. Measured $\log D$ at pH 7.4, pK_a , plasma protein binding (f_{up}), *in vitro* intestinal permeability from Ussing chamber experiments, biorelevant solubility and CYP3A recombinant enzyme kinetics (biphasic) and microsomal binding ($f_{u_{mic}}$) were used in model building^{18,21}.

Regional permeability and cumulative dissolution of an immediate-release (IR) formulation of venetoclax were mechanistically predicted using the mechanistic permeability (MechPeff) and Wang and Flanagan diffusion-layer sub-models (DLM) within the Simcyp Advanced Dissolution, Absorption and Metabolism (ADAM) model^{19,22,23}.

DLM allows extrapolation of *in vivo* dissolution rate from the IR formulation in a gastro-intestinal segment over time^{6,19,22,23}:

$$DR(t) = -NS \frac{D_{eff}}{h_{eff}(t)} 4\pi a(t) (a(t) + h_{eff}(t)) (S_{surf}(t) - C_{bulk}(t)) \quad (3)$$

where $DR(t)$ is the rate of dissolution at time t ; D_{eff} is the effective diffusion coefficient; $h_{eff}(t)$ is the thickness of the hydrodynamic boundary layer at time t ; $a(t)$ is the particle radius at time t ; $C_{bulk}(t)$ is the concentration of dissolved drug in bulk solution at time t , and $S_{surf}(t)$ is the saturation solubility at the particle surface at time t . H_{eff} was estimated using the Hintz-Johnson sub-model and D_{eff} was calculated within Simcyp based on molecular weight^{6,19,23}. Precipitation of venetoclax was estimated using Model 2, which takes into account meta-stable supersaturated concentrations. In this model, the intrinsic solubility was set to the amorphous solubility. The critical supersaturation ratio was set to 1, as venetoclax will precipitate as amorphous GLPS particles, which should remain amorphous throughout the timeframe it resides in the gastrointestinal tract (see Supporting Material). The precipitation rate constant was set to very low (i.e. 0.0001 h^{-1}) to help maintain concentrations at the amorphous solubility. Sensitivity analysis was performed with respect to particle size from 200 nm to 20 μm . This range was selected based on experience with GLPS particles that typically do not go beyond the upper value defined, as well as polarized light microscopy images confirming this observation. The sensitivity analysis did not indicate a

significant effect of particle size on the fraction absorbed (see Supporting Material), therefore the particle size was set to a default value of 10 μm . All input data are summarized in table 2.

The MechPeff model accounts for regional differences in effective permeability ($P_{eff,man}$) based on knowledge of regional GI morphology and physiology, as well as, inter-individual variability in these parameters^{22,24,25}. Here the intrinsic permeability ($P_{trans,0}$) used in the MechPeff model was calibrated against the corresponding measured jejunum I $P_{eff,man}$ determined using the Ussing chamber assay. Assuming that transcellular permeability dominates (low paracellular and unstirred boundary layer permeability), the on-screen $P_{trans,0}$ was manually adjusted to reproduce the jejunum $P_{eff,man}$ value. This $P_{trans,0}$ value was then used in the software to predict the relevant $P_{eff,man}$ in the other regions of the intestine. While it has been shown *in vitro* that venetoclax is a substrate of P-gp and BCRP, kinetic parameters could not be measured for incorporation in the model due to low intrinsic solubility of this compound. As rat Ussing chamber experiments were conducted in the absence of any active transport inhibitors, the measured permeability should account for active and passive processes, albeit not accounting for species differences in transporter expression.

A measured value was not available for the unbound fraction of drug within the enterocyte, therefore, measured unbound fraction in human liver microsome ($f_{u,mic}$) was used as a surrogate for $f_{u,Gut}$ in the model.

The Rodgers and Rowland method (Method 2) was used to predict the volume of distribution at steady state (V_{ss}) as it performed better than the Poulin and Theil method (Method 1) to predict the estimated clinical V_{ss} ²⁶⁻²⁸. Though venetoclax was not dosed intravenously in the clinic, a population PK analysis of the PK parameters in fasting healthy human volunteers indicated that the V_{ss}/F is 118 L²⁹. For an average individual weighing 74 Kg, this translates to a V_{ss}/F of 1.6 L/Kg. Based on the physicochemical properties of venetoclax, as well as its low permeability, bioavailability in the fasted state is expected to be around 10%. Therefore, the clinical V_{ss} is estimated to be approximately 0.2 L/Kg, which is in agreement with the prediction obtained from the Rodgers and Rowland method. Furthermore, the geometric mean of V_{ss} across three preclinical species (rat, dog and monkey) corrected for plasma

binding was determined to be 0.3 L/kg, which is also in agreement with the value predicted using Method 2³⁰.

In vitro measurements in human recombinant enzymes indicate that venetoclax is primarily metabolized via the CYP3A4/5²¹. Following oral administration in human, the major route of elimination of venetoclax (parent compound) was biliary/fecal excretion of the parent and metabolites²¹, likely related to its incomplete gastrointestinal absorption resulting from its low permeability and solubility (Table 1). In the PBPK model, venetoclax elimination of the absorbed fraction was assumed to be exclusively through CYP3A4/5 metabolism.

The initial PBPK model was used to simulate 10 trials of 24 subjects dosed with 100 mg venetoclax under fasting conditions.

PBPK Model Verification

The ability of the PBPK model to correctly predict the observed clinical food effect was verified against the results of a single food effect study in 10 trials of 24 healthy volunteers (240 individuals) using 100 mg under fed (low- and high-fat meal) conditions as previously described³¹. The predicted AUC_{∞} and C_{max} ratios were compared to the respective observed parameters and a 0.8- to 1.25-fold range was used as stringent criteria for model verification^{32,33}.

The ability of the PBPK model to correctly predict potential drug-drug interactions (DDIs) was verified against two independent clinical studies assessing the strong CYP3A inhibitor ketoconazole⁵ and the strong CYP3A inducer, multiple dose rifampin⁴. Verification of the venetoclax PBPK model was carried out using identical study design as the clinical ketoconazole and rifampin studies^{4,5}. Simulations were carried out in 10 trials of 12 healthy volunteers using 50 mg and 200 mg venetoclax with the default, built-in ketoconazole 400 mg QD and rifampin 600 mg QD (MD) PBPK compound files available in the Simcyp Simulator, respectively. The predicted AUC_{∞} and C_{max} ratios were compared to the respective observed parameters and a 0.8- to 1.25-fold range was used as stringent criteria for model verification^{32,33}.

Results

Venetoclax has high plasma protein binding, with a f_{up} value of 1.3×10^{-5} as determined by equilibrium dialysis. Ussing chamber results showed that venetoclax has a low apparent permeability of 1.02×10^{-6} cm/s in rat, which translates to a $P_{eff,man}$ value of 0.3×10^{-4} cm/s in human jejunum. The amorphous solubility of venetoclax was measured to be $4.5 \mu\text{g/mL}$ under neutral conditions and $13 \mu\text{g/mL}$ in acidic conditions, all in the presence of polymer to help promote GLPS formation (Table 2). Under simulated intestinal fluid conditions, amorphous solubilities ranged between $20 \mu\text{g/mL}$ and $55 \mu\text{g/mL}$ depending on fasted vs. fed conditions. Crystallization tendency was observed for venetoclax using a polarized light microscope and found to be stable as GLPS particles for at least 24 hours (see Supporting Material). Based on these observations, venetoclax is not believed to crystallize under physiological conditions at a physiological timeframe (24 hours) (Figure 1). In terms of rate of crystallization, venetoclax would be considered very slow if classified as part of the amorphous classification system³⁴.

Model Development and Evaluation

The performance of the initial venetoclax PBPK model was assessed by simulating plasma concentration-time profile following a single 100 mg dose in fasted female healthy volunteer subjects. The model under-predicted the observed plasma venetoclax exposure and over-predicted the observed T_{max} ³¹. As venetoclax is known to be a substrate of efflux transporters²¹, and the correlation used to determine the $P_{eff,man}$ from rat Ussing chamber experiments does not account for the inter-species differences in active processes, there was uncertainty in the initial permeability ($P_{trans,0}$) value used in the MechPeff model. A parameter estimation approach was utilized to optimize the $P_{trans,0}$ value resulting in a jejunum $P_{eff,man}$ value of 0.98×10^{-4} cm/s instead of the measured value of 0.3×10^{-4} cm/s. The optimized PBPK model was then able to capture the plasma PK profile of venetoclax in fasted female subjects (Figure 2) and the model predicted the observed PK parameters within the 0.8- to 1.25-fold range criteria for model verification (Table 3).

Model Verification

The ability of the PBPK model to capture the clinically-observed 3.4-fold (low-fat diet) to 5.2-fold (high-fat diet) increase in venetoclax exposure (C_{max} and AUC) was evaluated in the presence of food³¹.

Simulation of plasma concentration-time profiles following a single 100 mg dose in fed female subjects successfully captured the observed fold increase following a low-fat meal condition (Figure 3).

Comparison of the geometric mean of the observed PK parameters following a low-fat diet in healthy female volunteers was in good agreement with the predicted geometric mean of the PK parameters; within 0.81- to 0.92-fold (Table 4). The current model was not able to capture the observed fold increase following a high-fat meal condition (~5-fold) (data not shown)³¹.

The venetoclax model was further verified against independent clinical studies assessing the effect of the strong CYP3A inhibitor ketoconazole (400 mg QD) and the strong CYP3A inducer rifampicin (600 mg QD)^{4,5}. The model described the ratio of AUC and C_{max} of venetoclax in the presence of ketoconazole within 0.81- and 0.82-fold of the observed ratios, respectively (Table 5). Furthermore, the model was able to adequately capture the effect of the CYP3A inducer rifampin on plasma venetoclax concentrations within 0.98- and 1.21-fold of the observed AUC and C_{max} ratios (Table 5). This data indicate that the model can successfully capture the mechanism of CYP3A metabolism of venetoclax.

Discussion

The PBPK model developed here using a middle-out approach was able to capture mechanistically the disposition of the BCL-2 inhibitor, venetoclax, while accounting for dissolution, permeability and enzymatic metabolism. Verification with clinical data from healthy volunteer subjects confirmed that the model predicts the disposition of venetoclax, as well as, the observed food effect following a low-fat diet. The PBPK model was further verified for its ability to accurately predict the effects of strong CYP3A inhibitors and inducers on venetoclax PK within the stringent 0.8- to 1.25-fold range for model verification^{29,33}. As this model could be verified for CYP3A interactions ranging from strong inhibition to strong induction, it can have future application in assessing potential interaction with mild and intermediate modulators of CYP3A in healthy volunteers.

While a PBPK model has previously been used to describe the disposition of venetoclax using clinical dissolution data¹³, the food effect was not captured mechanistically (i.e. using *in vitro* data for solubility and dissolution), instead, an empirical approach was used where the profile was captured through dose adjustment. An important aim of this work was to capture the venetoclax PK profile under fasted and fed conditions by correctly incorporating the dissolution and absorption mechanisms of venetoclax within the PBPK model. Venetoclax can precipitate as phase separated drug-rich amorphous particles, described more recently in the literature as glass-liquid phase separation (GLPS)³⁵. GLPS occurs for certain molecules after concentrations reach above the amorphous solubility of the drug and is a concentration which represents the highest driving force achievable for flux through the intestinal epithelium¹². Therefore, if GLPS can be maintained *in vivo*, it may also represent the concentrations that will help overcome other barriers that might be present (e.g. efflux) or represent concentrations that will be available to be taken up by intestinal uptake transporters¹¹. Therefore, it is imperative to appropriately account for the maximum available concentrations that can be reached in the GI tract. For venetoclax, the amorphous solubility in pure aqueous conditions was the most relevant measurement to use in the PBPK model for this particular type of clinical/commercial formulation (ASD). Additionally, it was also critical to appropriately describe the precipitation behavior within the model to reflect the *in vivo* conditions (i.e. maintenance of GLPS).

One limitation of using amorphous solubility within the Simcyp PBPK platform is that the rate of replenishment of amorphous drug back into available luminal concentrations is not considered. For a compound with a low net permeability (and low expected absorption), however, this replenishment rate may be negligible and maintenance of concentrations at the amorphous solubility may be representative of the *in vivo* situation. While the model captures the food effect observed following a low-fat diet, it could not adequately account for the greater than 5-fold food effect observed following a high-fat diet. Given the high lipophilicity of venetoclax, the observed food effect following a high-fat meal may arise from increased solubilization of the hydrophobic venetoclax molecule by not only forming bile salt micelles, but also by dissolving the molecule in the lipophilic phase. While the solubility in the classical FeSSIF buffer previously described in the literature³⁶ was used in the current model to simulate the biorelevant solubility, the composition of this medium may be more reflective of a low-fat diet, rather than a high-fat meal,

especially in the presence of a highly lipophilic compound³⁶⁻³⁸, Therefore, the *in vitro* biorelevant data used in the current model may only sufficiently explain the food effect following intake of a meal with low fat composition. An additional mechanism, which may contribute to increased systemic exposure of venetoclax following a high-fat diet may be lymphatic absorption. Here, mechanistic modeling of the biorelevant ASD solubility accounts for the effect of surfactants in the formulation, however, it does not take into account the additional role of lymphatic absorption of venetoclax. The mechanism of lymphatic absorption could not be adequately captured using the models currently available within Simcyp Version 15. The impact of fatty acids and lipid particles on absorption was demonstrated *in vitro* where permeability of venetoclax was measured using a simulated lymphatic absorption model (data not shown). In this model a synthetic approximation of lymphatic fluid consisting of a simulated chylomicron created to mimic the reported lipid composition of chylomicrons found in human lymph was used in the absorption chamber of the Ussing apparatus³⁹ (further details of the methodology are provided in the Appendix 2). The results indicated an increase in permeability of venetoclax by approximately 3-fold, suggesting increased exposure in the presence of lipid particles and fatty components of a high-fat meal.

Several biorelevant dissolution methods have been described in the literature in an attempt to predict *in vivo* relevant concentrations^{8,40}. Typical United States Pharmacopeia (USP) methods fall short of predicting these concentrations correctly due to lack of an absorptive compartment creating the appropriate sink that mimics *in vivo* absorption. Additionally, the recommended 900 mL volumes are not representative of water and GI fluid present in the gastrointestinal lumen (assumed to be between 130 and 250 mL). Conventional six-vessel USP dissolution methods are generally run at a single pH whereas biorelevant methods attempt to capture the pH shift from low pH in the stomach (1-3) to small intestinal pH (5-6.8). An alternate approach was developed by Gao *et al.* (i.e. pH dilution) which attempts to capture biorelevant dissolution of ASD formulations over a range of pH mimicking the GI physiology⁸. pH dilution aims to appropriately account for GI fluid volumes, pH shifts and residence time as a formulation moves through the GI tract. Typically, pH dilution is a more appropriate method for evaluating supersaturating formulations like venetoclax compared to typical USP dissolution methods. However, the use of pH dilution data would only allow a semi-mechanistic approach where user-input segmental dissolution data would over-write the mechanistic simulation of segmental biorelevant solubility and dissolution within the

PBPK. Use of this data will require separate files with input for either fasted or fed state (solubility data from separate experiments run in FaSSIF and FeSSIF buffer), which is not ideal. The mechanistic approach described here demonstrates the use of *in vitro* data to successfully predict the disposition and observed food effect of a BCS class IV, ASD formulation using PBPK modeling.

Conclusion

The application of PBPK models to simulating the pharmacokinetics and disposition of compounds with high thermodynamic solubility and permeability has been extensively described in the literature, while models describing the disposition of BCS class IV compounds that require an ASD formulation to obtain adequate *in vivo* absorption and dissolution are lacking. This manuscript describes the development of a mechanistic PBPK model using *in vitro* data on amorphous solubility and dissolution of the low solubility and low permeability compound, venetoclax to correctly capture the human PK profile and food effect. Furthermore, the inclusion of *in vitro* CYP3A kinetics data correctly captured the elimination profile of this compound while allowing prediction of potential CYP3A-related drug interactions. The PBPK model can have future applications in predicting un-tested drug interactions, especially those that may primarily occur within the gastrointestinal tract and is one of the first examples of a model that mechanistically captures the absorption and disposition of an ASD formulation.

Supporting Information

This article contains supplementary material available from the authors upon request or via the internet.

ACCEPTED MANUSCRIPT

References

1. Souers AJ, Levenson JD, Boghaert ER, Ackler SL, Catron ND, Chen J, Dayton BD, Ding H, Enschede SH, Fairbrother WJ, Huang DC, Hymowitz SG, Jin S, Khaw SL, Kovar PJ, Lam LT, Lee J, Maecker HL, Marsh KC, Mason KD, Mitten MJ, Nimmer PM, Oleksijew A, Park CH, Park CM, Phillips DC, Roberts AW, Sampath D, Seymour JF, Smith ML, Sullivan GM, Tahir SK, Tse C, Wendt MD, Xiao Y, Xue JC, Zhang H, Humerickhouse RA, Rosenberg SH, Elmore SW 2013. ABT-199, a potent and selective BCL-2 inhibitor, achieves antitumor activity while sparing platelets. *Nat Med* 19(2):202-208.
2. Roberts AW, Davids MS, Pagel JM, Kahl BS, Puvvada SD, Gerecitano JF, Kipps TJ, Anderson MA, Brown JR, Gressick L, Wong S, Dunbar M, Zhu M, Desai MB, Cerri E, Heitner Enschede S, Humerickhouse RA, Wierda WG, Seymour JF 2016. Targeting BCL2 with Venetoclax in Relapsed Chronic Lymphocytic Leukemia. *N Engl J Med* 374(4):311-322.
3. Davids MS, Roberts AW, Seymour JF, Pagel JM, Kahl BS, Wierda WG, Puvvada S, Kipps TJ, Anderson MA, Salem AH, Dunbar M, Zhu M, Peale F, Ross JA, Gressick L, Desai M, Kim SY, Verdugo M, Humerickhouse RA, Gordon GB, Gerecitano JF 2017. Phase I First-in-Human Study of Venetoclax in Patients With Relapsed or Refractory Non-Hodgkin Lymphoma. *J Clin Oncol* 35(8):826-833.
4. Agarwal SK, Hu B, Chien D, Wong SL, Salem AH 2016. Evaluation of Rifampin's Transporter Inhibitory and CYP3A Inductive Effects on the Pharmacokinetics of Venetoclax, a BCL-2 Inhibitor: Results of a Single- and Multiple-Dose Study. *J Clin Pharmacol* 56(11):1335-1343.
5. Agarwal SK, Salem AH, Danilov AV, Hu B, Puvvada S, Gutierrez M, Chien D, Lewis LD, Wong SL 2017. Effect of ketoconazole, a strong CYP3A inhibitor, on the pharmacokinetics of venetoclax, a BCL-2 inhibitor, in patients with non-Hodgkin lymphoma. *Br J Clin Pharmacol* 83(4):846-854.
6. Cristofolletti R, Dressman JB 2016. Bridging the Gap Between In Vitro Dissolution and the Time Course of Ibuprofen-Mediating Pain Relief. *J Pharm Sci* 105(12):3658-3667.
7. Kesisoglou F, Hermans A, Neu C, Yee KL, Palcza J, Miller J 2015. Development of In Vitro-In Vivo Correlation for Amorphous Solid Dispersion Immediate-Release Suvorexant Tablets and Application to Clinically Relevant Dissolution Specifications and In-Process Controls. *J Pharm Sci* 104(9):2913-2922.
8. Gao Y, Carr RA, Spence JK, Wang WW, Turner TM, Lipari JM, Miller JM 2010. A pH-dilution method for estimation of biorelevant drug solubility along the gastrointestinal tract: application to physiologically based pharmacokinetic modeling. *Mol Pharm* 7(5):1516-1526.
9. Newman A, Knipp G, Zografi G 2012. Assessing the performance of amorphous solid dispersions. *J Pharm Sci* 101(4):1355-1377.
10. Taylor LS, Zhang GG 2016. Physical chemistry of supersaturated solutions and implications for oral absorption. *Adv Drug Deliv Rev* 101:122-142.
11. Beig A, Fine-Shamir N, Lindley D, Miller JM, Dahan A 2017. Advantageous Solubility-Permeability Interplay When Using Amorphous Solid Dispersion (ASD) Formulation for the BCS Class IV P-gp Substrate Rifaximin: Simultaneous Increase of Both the Solubility and the Permeability. *AAPS J* 19(3):806-813.
12. Raina SA, Zhang GG, Alonzo DE, Wu J, Zhu D, Catron ND, Gao Y, Taylor LS 2015. Impact of Solubilizing Additives on Supersaturation and Membrane Transport of Drugs. *Pharm Res* 32(10):3350-3364.
13. Freise KJ, Shebley M, Salem AH 2017. Quantitative Prediction of the Effect of CYP3A Inhibitors and Inducers on Venetoclax Pharmacokinetics Using a Physiologically Based Pharmacokinetic Model. *J Clin Pharmacol* 57(6):796-804.

14. Kalvass JC, Maurer TS, Pollack GM 2007. Use of plasma and brain unbound fractions to assess the extent of brain distribution of 34 drugs: comparison of unbound concentration ratios to in vivo p-glycoprotein efflux ratios. *Drug Metab Dispos* 35(4):660-666.
15. Kalvass JC, Maurer TS 2002. Influence of nonspecific brain and plasma binding on CNS exposure: implications for rational drug discovery. *Biopharm Drug Dispos* 23(8):327-338.
16. Kim JS, Mitchell S, Kijek P, Tsume Y, Hilfinger J, Amidon GL 2006. The suitability of an in situ perfusion model for permeability determinations: utility for BCS class I biowaiver requests. *Mol Pharm* 3(6):686-694.
17. Riethorst D, Baatsen P, Remijn C, Mitra A, Tack J, Brouwers J, Augustijns P 2016. An In-Depth View into Human Intestinal Fluid Colloids: Intersubject Variability in Relation to Composition. *Mol Pharm* 13(10):3484-3493.
18. Avdeev A. 2012. Solubility, Permeability and Charge State. . Absorption and Drug Development, 2nd ed., Hoboken, New Jersey: John Wiley & Sons.
19. Jamei M, Dickinson GL, Rostami-Hodjegan A 2009. A framework for assessing inter-individual variability in pharmacokinetics using virtual human populations and integrating general knowledge of physical chemistry, biology, anatomy, physiology and genetics: A tale of 'bottom-up' vs 'top-down' recognition of covariates. *Drug Metab Pharmacokinet* 24(1):53-75.
20. Tsamandouras N, Rostami-Hodjegan A, Aarons L 2015. Combining the 'bottom up' and 'top down' approaches in pharmacokinetic modelling: fitting PBPK models to observed clinical data. *Br J Clin Pharmacol* 79(1):48-55.
21. Kikuchi R, Shebly M, Bow D, Carr R, Nijssen M, De Morai S 2016. In vitro characterization of drug metabolizing enzymes and transporters to enable a mechanistic drug-drug interaction assessment of venetoclax. . Presented at: 11th International ISSX Meeting Busan, Korea:June 12-16.
22. Pade D, Jamei M, Rostami-Hodjegan A, Turner DB 2017. Application of the MechPeff model to predict passive effective intestinal permeability in the different regions of the rodent small intestine and colon. *Biopharm Drug Dispos* 38(2):94-114.
23. Wang J, Flanagan DR 1999. General solution for diffusion-controlled dissolution of spherical particles. 1. Theory. *J Pharm Sci* 88(7):731-738.
24. Lennernas H 2014. Human in vivo regional intestinal permeability: importance for pharmaceutical drug development. *Mol Pharm* 11(1):12-23.
25. Sugano K 2009. Theoretical investigation of passive intestinal membrane permeability using Monte Carlo method to generate drug-like molecule population. *Int J Pharm* 373(1-2):55-61.
26. Berezhkovskiy LM 2004. Volume of distribution at steady state for a linear pharmacokinetic system with peripheral elimination. *J Pharm Sci* 93(6):1628-1640.
27. Poulin P, Theil FP 2002. Prediction of pharmacokinetics prior to in vivo studies. 1. Mechanism-based prediction of volume of distribution. *J Pharm Sci* 91(1):129-156.
28. Rodgers T, Rowland M 2006. Physiologically based pharmacokinetic modelling 2: predicting the tissue distribution of acids, very weak bases, neutrals and zwitterions. *J Pharm Sci* 95(6):1238-1257.
29. Jones AK, Freise KJ, Agarwal SK, Humerickhouse RA, Wong SL, Salem AH 2016. Clinical Predictors of Venetoclax Pharmacokinetics in Chronic Lymphocytic Leukemia and Non-Hodgkin's Lymphoma Patients: a Pooled Population Pharmacokinetic Analysis. *AAPS J* 18(5):1192-1202.
30. Waters NJ, Lombardo F 2010. Use of the Oie-Tozer model in understanding mechanisms and determinants of drug distribution. *Drug Metab Dispos* 38(7):1159-1165.
31. Salem AH, Agarwal SK, Dunbar M, Nuthalapati S, Chien D, Freise KJ, Wong SL 2016. Effect of Low- and High-Fat Meals on the Pharmacokinetics of Venetoclax, a Selective First-in-Class BCL-2 Inhibitor. *J Clin Pharmacol* 56(11):1355-1361.

32. Jones HM, Chen Y, Gibson C, Heimbach T, Parrott N, Peters SA, Snoeys J, Upreti VV, Zheng M, Hall SD 2015. Physiologically based pharmacokinetic modeling in drug discovery and development: a pharmaceutical industry perspective. *Clin Pharmacol Ther* 97(3):247-262.
33. Wagner C, Pan Y, Hsu V, Grillo JA, Zhang L, Reynolds KS, Sinha V, Zhao P 2015. Predicting the effect of cytochrome P450 inhibitors on substrate drugs: analysis of physiologically based pharmacokinetic modeling submissions to the US Food and Drug Administration. *Clin Pharmacokinet* 54(1):117-127.
34. Baird JA, Van Eerdenbrugh B, Taylor LS 2010. A classification system to assess the crystallization tendency of organic molecules from undercooled melts. *J Pharm Sci* 99(9):3787-3806.
35. Mosquera-Giraldo LI, Taylor LS 2015. Glass-liquid phase separation in highly supersaturated aqueous solutions of telaprevir. *Mol Pharm* 12(2):496-503.
36. Dressman JB, Reppas C 2000. In vitro-in vivo correlations for lipophilic, poorly water-soluble drugs. *Eur J Pharm Sci* 11 Suppl 2:S73-80.
37. Vertzoni M, Fotaki N, Kostewicz E, Stippler E, Leuner C, Nicolaidis E, Dressman J, Reppas C 2004. Dissolution media simulating the intraluminal composition of the small intestine: physiological issues and practical aspects. *J Pharm Pharmacol* 56(4):453-462.
38. Xie X, Cardot JM, Garrait G, Thery V, El-Hajji M, Beyssac E 2014. Micelle dynamic simulation and physicochemical characterization of biorelevant media to reflect gastrointestinal environment in fasted and fed states. *Eur J Pharm Biopharm* 88(2):565-573.
39. Tso P, Balint JA 1986. Formation and transport of chylomicrons by enterocytes to the lymphatics. *Am J Physiol* 250(6 Pt 1):G715-726.
40. Tsume Y, Matsui K, Searls AL, Takeuchi S, Amidon GE, Sun D, Amidon GL 2017. The impact of supersaturation level for oral absorption of BCS class IIb drugs, dipyridamole and ketoconazole, using in vivo predictive dissolution system: Gastrointestinal Simulator (GIS). *Eur J Pharm Sci* 102:126-139.

Figure Legends

Figure 1. Illustration of venetoclax solubility and precipitation behavior – initial rapid supersaturation of venetoclax to its amorphous solubility occurs at 4.6 µg/mL (critical supersaturation concentration, CSC). Above this concentration, GPLS particles form and replenish amorphous drug to help maintain concentrations at the amorphous solubility. Data above describing the slow precipitation rate (PRC) of venetoclax allows maintenance at the CSC.

Figure 2 – Mean simulated (solid line) and observed (circles) plasma venetoclax concentration-time profiles in fasted, female healthy volunteer subjects (10 trials of 24 individuals) following administration of a single 100-mg venetoclax dose. Dashed lines represent the 5th and 95th percentiles. The different colors represent different subjects.

Figure 3 – Mean simulated (solid line) and observed (circles) plasma venetoclax concentration-time profiles in fed, female healthy volunteer subjects (10 trials of 24 individuals) following administration of a single 100-mg venetoclax dose. Dashed lines represent the 5th and 95th percentiles. The different colors represent different subjects.

Tables

Table 1. pH-modified bio-relevant amorphous solubility data used for parameter estimation in SIVA.

Measured pH	Surfactant Concentration (mM)	Critical Micelle Concentration (mM)	Experimental in vitro Solubility ($\mu\text{g/mL}$) \pm SD
5.3	3.75	3	20.7 ± 0.8
6.9	3.75	3	33.7 ± 13.5
5.3	18.75	3	26.4 ± 0.2
6.9	18.75	3	54.6 ± 2

Table 2. Input data values for venetoclax mechanistic PBPK model.

Parameter	Input value	Source
Physicochemical Properties		
Molecular Weight (g/mol)	868.44	
Log P _{o:w}	8	Predicted in Simcyp from experimentally determine LogD of 5.4 at pH 7.4 ¹
Compound Type	Ampholyte	Experimentally determined
pKa1 (acid)	3.4	Experimentally determined
pKa2 (base)	10.3	Experimentally determined
Blood to plasma ratio (B:P)	0.574	Experimentally determined ²
Fraction unbound in plasma (f _{u,p})	1.3 x 10 ⁻⁵	Experimentally determined
Permeability		
P _{eff,man} (10 ⁻⁴ cm/s) duodenum	0.49	Predicted using the Simcyp mechanistic P _{eff} (MechPeff) model ³ from the experimentally determined P _{eff,man} of 0.3 x 10 ⁻⁴ cm/s, optimized to 0.98 x 10 ⁻⁴ cm/s.
P _{eff,man} (10 ⁻⁴ cm/s) jejunum I	0.98	
P _{eff,man} (10 ⁻⁴ cm/s) jejunum II	0.69	
P _{eff,man} (10 ⁻⁴ cm/s) ileum I-III	0.31	
P _{eff,man} (10 ⁻⁴ cm/s) ileum IV	0.29	
P _{eff,man} (10 ⁻⁴ cm/s) colon	0.20	
Solubility and Dissolution from immediate release		
Amorphous solubility pH profile (µg/mL) (used in model to calculate S _{surf})	From 13 (pH 1) to 4.5 (pH 7.4)	Experimentally determined
Logarithm of bile midelle:buffer partition coefficient (logK _{m:w})	Neutral = 0.774 Ion = 3.32	Obtained using SIVA

Critical supersaturation ratio	1	Experimentally estimated
Precipitation rate constant	0.0001	Experimentally estimated
Particle radius (μm)	10	Simcyp default
Particle H_{eff} (μm)	1	Simcyp default
<i>Distribution and Elimination</i>		
V _{ss} (L/Kg)	0.21	Method 2 ⁴
<i>CYP3A4 – 4-OH pathway</i>		
V _{max} (pmol/min/pmol isoform)	3.468	Experimentally determined ²
K _m (μM)	4.632	Experimentally determined ²
$f_{u_{mic}}$	0.0006	Calculated from experimentally determined $f_{u_{mic}}$ based on protein content ⁵
<i>CYP3A4 – α-OH pathway</i>		
CL _{int} ($\mu\text{L}/\text{min}/\text{pmol}$ isoform)	0.163	Experimentally determined ²
$f_{u_{mic}}$	0.0006	Calculated from experimentally determined $f_{u_{mic}}$ based on protein content ⁵
<i>CYP3A5 – 4-OH pathway</i>		
CL _{int} ($\mu\text{L}/\text{min}/\text{pmol}$ isoform)	0.062	Experimentally determined ²
$f_{u_{mic}}$	0.0006	Calculated from experimentally determined $f_{u_{mic}}$ based on protein content ⁵

Table 3 – Comparison of predicted and observed venetoclax PK parameters in fasted healthy subjects following a 100-mg dose.

Parameter	Predicted (Geometric Mean \pm SD)	Observed (Geometric Mean)⁶	Ratio (Predicted:Observed)
AUC _{0-∞} ($\mu\text{g/mL}\cdot$ hr)	2.25 \pm 1.62	2.08	1.08
C _{max} ($\mu\text{g/mL}$)	0.16 \pm 0.06	0.15	1.01
t _{max} (hours)	4.37 \pm 1.35	4.3	1.02

Table 4 – Comparison of predicted and observed venetoclax PK parameters in fed healthy subjects following a 100-mg dose.

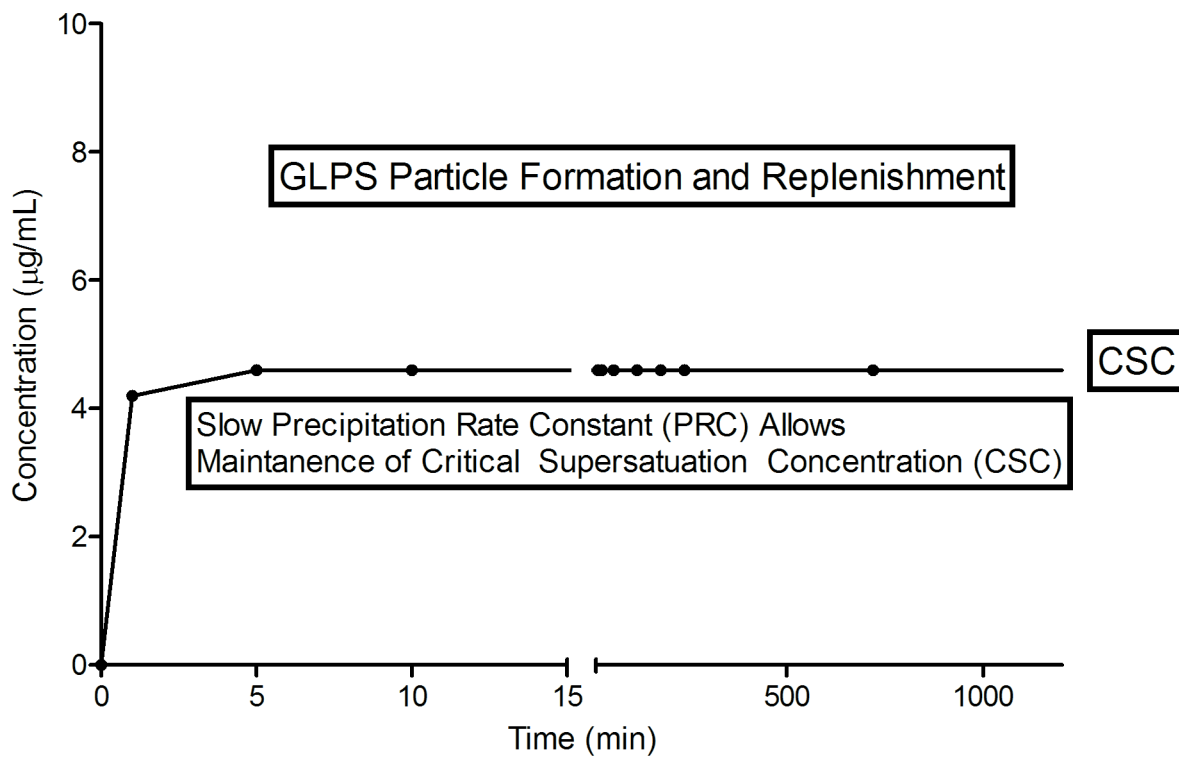
Parameter	Predicted (Geometric Mean \pm SD)	Observed (Geometric Mean) ⁶		Ratio (Predicted:Observed)	
		Low-fat Diet	High-fat Diet	Low-fat Diet	High-fat Diet
$AUC_{0-\infty}$ ($\mu\text{g/mL}\cdot\text{hr}$)	6.10 ± 4.55	7.1	10.54	0.86	0.58
C_{max} ($\mu\text{g/mL}$)	0.40 ± 0.16	0.5	0.78	0.81	0.51
t_{max} (hr)	5.60 ± 1.60	6.1	6.0	0.92	0.93

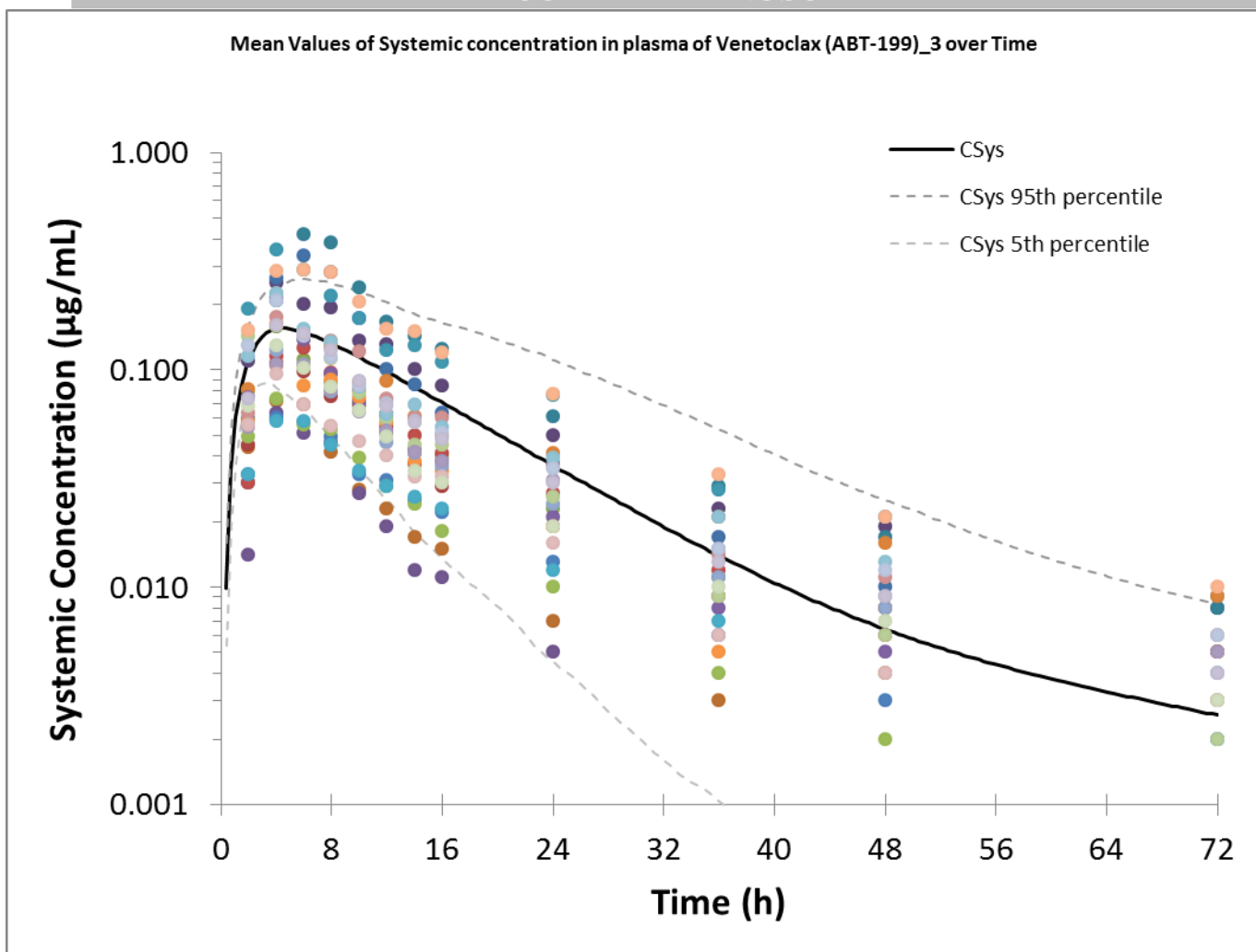
Table 5 – Comparison of predicted and observed venetoclax PK parameters ratio in fed healthy subjects when administered with ketoconazole and rifampicin.

Parameter	Ketoconazole (400 mg QD)			Rifampin (600 mg QD)		
	<i>Predicted (geometric mean)</i>	<i>Observed (geometric mean)⁷</i>	<i>Ratio (Predicted: Observed)</i>	<i>Predicted (geometric mean)</i>	<i>Observed (geometric mean)⁸</i>	<i>Ratio (Predicted: Observed)</i>
AUC_{0-∞} Ratio	5.16 ± 3.03	6.40	0.81	0.20 ± 0.08	0.2	0.98
C_{max} Ratio	1.89 ± 0.34	2.32	0.82	0.36 ± 0.12	0.3	1.21

1. Avdeev A. 2012. Solubility, Permeability and Charge State. . Absorption and Drug Development, 2nd ed., Hoboken, New Jersey: John Wiley & Sons.
2. Kikuchi R, Shebly M, Bow D, Carr R, Nijssen M, De Morai S 2016. In vitro characterization of drug metabolizing enzymes and transporters to enable a mechanistic drug-drug interaction assessment of venetoclax. . Presented at: 11th International ISSX Meeting Busan, Korea:June 12-16.
3. Pade D, Jamei M, Rostami-Hodjegan A, Turner DB 2017. Application of the MechPeff model to predict passive effective intestinal permeability in the different regions of the rodent small intestine and colon. *Biopharm Drug Dispos* 38(2):94-114.
4. Rodgers T, Rowland M 2006. Physiologically based pharmacokinetic modelling 2: predicting the tissue distribution of acids, very weak bases, neutrals and zwitterions. *J Pharm Sci* 95(6):1238-1257.
5. Austin RP, Barton P, Cockroft SL, Wenlock MC, Riley RJ 2002. The influence of nonspecific microsomal binding on apparent intrinsic clearance, and its prediction from physicochemical properties. *Drug Metab Dispos* 30(12):1497-1503.
6. Salem AH, Agarwal SK, Dunbar M, Nuthalapati S, Chien D, Freise KJ, Wong SL 2016. Effect of Low- and High-Fat Meals on the Pharmacokinetics of Venetoclax, a Selective First-in-Class BCL-2 Inhibitor. *J Clin Pharmacol* 56(11):1355-1361.
7. Agarwal SK, Salem AH, Danilov AV, Hu B, Puvvada S, Gutierrez M, Chien D, Lewis LD, Wong SL 2017. Effect of ketoconazole, a strong CYP3A inhibitor, on the pharmacokinetics of venetoclax, a BCL-2 inhibitor, in patients with non-Hodgkin lymphoma. *Br J Clin Pharmacol* 83(4):846-854.
8. Agarwal SK, Hu B, Chien D, Wong SL, Salem AH 2016. Evaluation of Rifampin's Transporter Inhibitory and CYP3A Inductive Effects on the Pharmacokinetics of Venetoclax, a BCL-2 Inhibitor: Results of a Single- and Multiple-Dose Study. *J Clin Pharmacol* 56(11):1335-1343.

Venetoclax Solubility and Precipitation Behavior





ACCEPTED

